ORIGINAL PAPER

Adjusting for Running-in: Extension of the Archard Wear Equation

Michael Varenberg[1] 🅾

Abstract

The Archard equation is widely employed to predict wear in engineering practice, but its use is usually restricted to the cases of sufficiently long wear duration, so the transient running-in behavior can be neglected with respect to the steady-state wear. To address this problem, here the steady state wear equation is extended into the running-in regime based on the bearing ratio curve representing the initial surface topography. This approach is verified using a unidirectional dry sliding of steel against PTFE and the extended equation is shown to be able to predict service life or to obtain wear coefficients regardless of the test duration if the initial surface topography is defined. It is also found that the bearing ratio curve can be efficiently approximated using the logistic function calibrated by four standard surface roughness parameters. This approximation proves to be more accurate than the widely used Gaussian normal distribution function.

Graphical Abstract
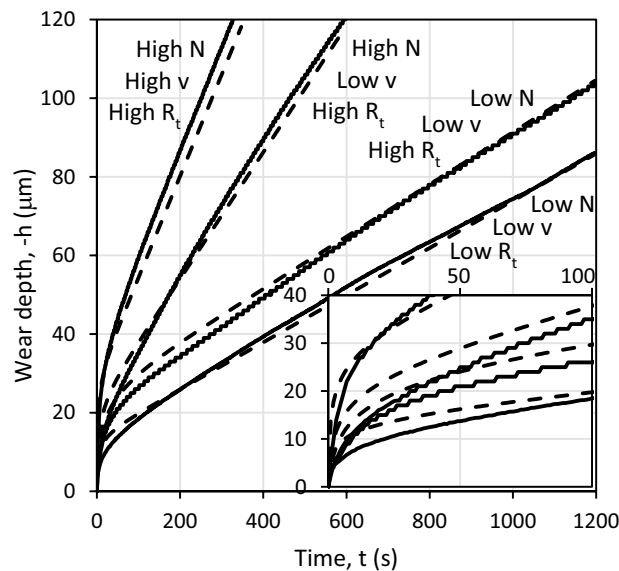
1 Introduction

Wear of two conformal surfaces rubbing against each other under either dry or lubricated conditions can be conveniently described using the Archard equation [1] that was developed assuming material removal at the contact points formed by plastic deformation. This equation postulates that the volume

✉ Michael Varenberg
  michael.varenberg@johncrane.com

1 John Crane Inc, Morton Grove, IL 60053, USA

worn per unit sliding distance is proportional to the applied load and is inversely proportional to the hardness of the softer surface, with the coefficient of proportionality being interpreted as the probability to generate a wear particle at a given contact point, the number of loading cycles needed to remove a material fragment, or the parameter correlated with the wear particle size [2]. Although the model was formulated based on an idealized depiction of adhesive wear, it is indifferent to the actual mechanism of material removal, and an identical equation can be derived for abrasive wear [2] and, possibly, for other types of wear [3] as well.

Due to its simplicity, the Archard equation is widely employed to predict material removal in engineering practice, with the applications ranging from wind turbine gearboxes [4] to prosthetic joints [5] to nano-electro-mechanical devices [6]. The predictions, however, can be considered accurate only if the material removal process lasts sufficiently long time, so the transient running-in behavior, observed until the stable surface conditions are established [2], can be neglected with respect to the steady-state wear [7]. It is obvious that in some cases, when large wear is not tolerated, such as in the applications involving thin coatings [8], this condition can be difficult to satisfy.

To address the problem of the transient running-in wear, surface roughness should be considered, as was recognized already in 1965 [9] (it is obvious that surface finish is not the only parameter affecting running-in, but all other factors, such as formation of transfer layers and loose wear particles, and chemical or physical interactions, are neglected to a first approximation). At present, the problem is usually solved by numerical modeling (see [10–12] as a few recent examples) based on statistical description of rough surfaces suggested by Greenwood and Williamson [13]. In this approach, purely elastic [13] or elastoplastic [14, 15] asperities of certain radius and areal density are assumed to have some height distribution (usually – Gaussian [12], less often – Weibull [11]), which yields a functional relationship between height/separation and truncation-based contact area needed to model the transient wear.

However, even if all the assumptions made are correct, which is not necessarily true [16], obtaining the rough surfaces' spectral moments required to execute the above models may become a challenging task due to uncertainties related to both measurement and computing methodologies [17–19]. On the other hand, without making any assumption about the studied surface, the bearing ratio curves (the Abbott-Firestone curves [20]), which are readily obtained in all modern profilers, can provide the required relationship between height and contact area. This ability calls to be explored in relation to wear studies. To this end, using the bearing ratio principle, we will develop here a straightforward analytical approach, somewhat in the spirit of the original "simple theory of mechanical wear", to extend Archard's famous steady-state wear equation into the transient running-in regime.

2 Analysis of Running-in Wear

Schematic of a typical wear curve is presented in Fig. 1 [21, 22], where all three stages of the wear evolution are shown. The initial running-in period is characterized by a high wear rate that is gradually reduced to a lower value as the system reaches the steady state. The steady state period lasts until increased friction, temperature, and/or vibration of worn parts induce the final stage of an accelerated wear that eventually leads to a failure. Here, we will focus on the analysis of wear during the initial running-in (breaking-in) period.

It is long known that contact between rough surfaces takes place at single asperities, so the real contact area is just a fraction of the nominal contact at any given moment, as defined by the applied load [13, 23]. However, in the process of steady state rubbing, each contact point is being formed and then reduced to zero as other contact points are established elsewhere in the surface [1]. Given that the average wear depth increases with a constant rate after the running-in period is finished, this means that 100% of the nominal contact area participate (though not simultaneously) in the steady state wear process.

These steady state surface conditions are characterized by a certain roughness that remains the same despite the surface continues to recess [24] and is defined by the relative motion, applied load, materials, and environment, while being different from and independent of the original topography that can be either roughened or smoothened [21]. This allows us to assume that the initial surface should be consumed completely from the highest to the lowest point during running-in and, hence, the total height of initial profile, R_t, may correspond to the wear depth at the end of the
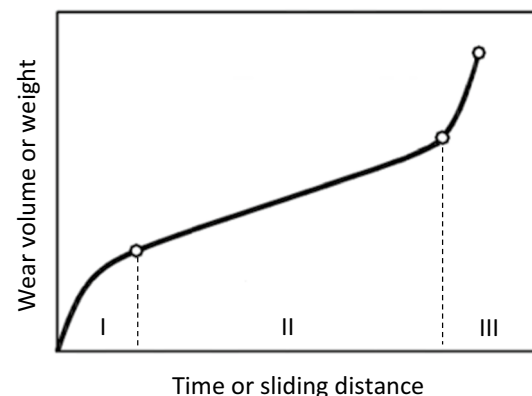

Fig. 1 Typical wear curve. (I) Running-in stage. (II) Steady-state wear stage. (III) Wear-out stage

running-in stage (regardless of whether the surface obtained in steady state is rougher or smoother). This idea is not new; in slightly different terms, it was formulated in [9]. The question is how fast the surface can recess to this point.

To answer this question, we will need to express the Archard equation, which was defined for 100% of the nominal contact area, in terms of the area that changes gradually from 0 to 100% as the material is removed from the highest to the lowest point of the initial surface. Applying a simple truncation approach, this can be achieved using the bearing ratio (material ratio) curve [20]. This curve shows the material ratio (fraction of truncation line lying within the material), Mr, which changes from 0 to 100%, as a function of height, h, at which this line is drawn, as presented in Fig. 2. Obviously, utilizing real measured bearing ratio curves would yield the most accurate results, but giving up on some accuracy to simplify the method significantly, we will approximate the bearing curve with a mathematical function.

Experimenting with different sigmoid functions, one can find that the logistic equation introduced originally to model population growth [25] is able to represent the bearing ratio curve with astonishing accuracy. Written in terms of the bearing ratio curve, the logistic function achieves the form

$$Mr = \frac{100}{1 + e^{a(b+h)}} \tag{1}$$

where the constants a and b describe the steepness of the curve and the height value of the curve's midpoint, respectively. Both constants can be found by calibrating this equation against the measured bearing ratio curve. Substituting the coordinates (h_1, Mr_1) and (h_2, Mr_2) that define the surface core height, R_k (Fig. 2), into Eq. (1), we obtain a system of two equations that yields

$$a = \frac{1}{R_k} \ln \left(\frac{100/Mr_1 - 1}{100/Mr_2 - 1} \right) \tag{2}$$

where R_k, Mr_1, and Mr_2 are the standard output parameters in modern profilers. To find b, which defines the curve's position along the h axis, we should recall that the logistic function goes from $-\infty$ to $+\infty$, so it must be truncated to represent the real surface profile. Given that the highest surface point most likely comes in contact first and is unequivocally defined, it would be best to place the origin there for the wear study. Hence, bearing in mind that b is the distance from the origin to the height at which the material ratio equals 50%, we can conclude that

$$b = R_{\delta c(0\%-50\%)} \tag{3a}$$

as shown in Fig. 2. In case the profiler cannot be configured to display $R_{\delta c(0\%-50\%)}$, the constant b can be computed by

$$b = R_{pk}^* + \frac{R_k}{2} \tag{3b}$$

as follows from Fig. 2, with R_{pk}^* and R_k also being standard parameters. It should be noted, though, that some simpler profilers may not offer the possibility to register the highest peak height, R_{pk}^*. In this case, the constant b can be approximated by

$$b \approx \frac{R_t}{2} \tag{3c}$$

but the more the surface departs from symmetry, containing mainly peaks or being mainly made up of valleys, the less accurate the approximation is.

Having Eq. (1) calibrated, we can now proceed to modifying the Archard wear equation [1]. In its classical form, this equation reads
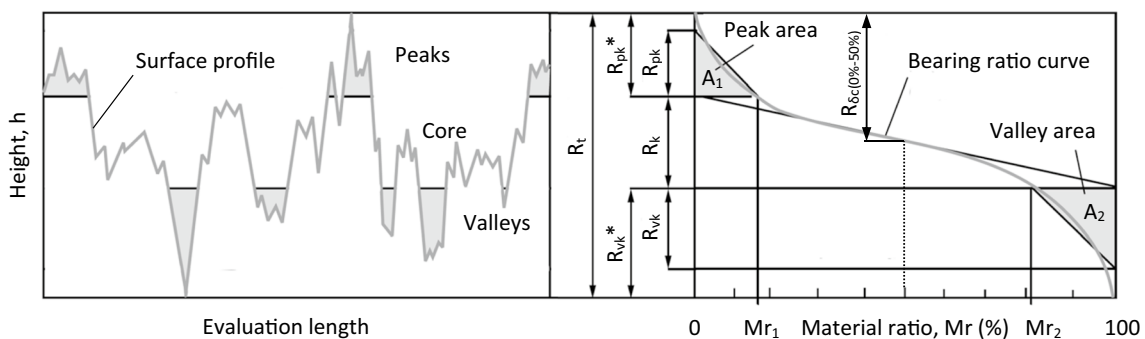

Fig. 2 Surface profile and bearing ratio curve. R_t, total roughness height. R_k, core roughness height. Mr_1 and Mr_2, smallest and greatest material ratios, respectively, at the limits of the core roughness. R_{pk}^*, highest peak height. R_{pk}, reduced peak height. A_1, equivalent triangle peak area. R_{vk}^*, deepest valley depth. R_{vk}, reduced valley depth. A_2, equivalent triangle valley area. $R_{\delta c(0\%-50\%)}$, height difference matching material ratios of 0 and 50%

$$V = K\frac{NL}{H} \tag{4}$$

where V is the worn volume, N is the normal load, L is the sliding distance, H is the hardness and K is the dimensionless wear coefficient. Normalizing this equation by the nominal contact area, replacing the sliding distance with the product of speed and time, hiding the hardness into the dimensional wear coefficient, recalling that we deal with the decreasing height (instead of the increasing depth), and, finally, expressing it in terms of the wear rate, we obtain

$$\frac{dh}{dt} = -kpv \tag{5}$$

where t is the time, k is the dimensional wear coefficient equal to K/H, p is the nominal contact pressure, and v is the sliding speed (with roughness remaining constant but neglected).

Equation (5) is valid for the steady state rubbing, which (per our simplifying analysis above) starts operating after the height measured from the point of first contact is reduced by the value of R_t, so that the highest surface point is located at the position of the initial material ratio of 100%. Using the same logic, we can think about what happens when the wear depth is smaller than R_t. If the dimensional wear coefficient and the sliding speed remain the same, the only parameter that can affect the wear rate is the pressure that should be inversely proportional to the contact area (provided that the normal load is also kept constant). Assuming that the contact area should change in accord with the changes in the material ratio, we can rewrite Eq. (5) as

$$\frac{dh}{dt} = -kpv\frac{100}{Mr} \tag{6}$$

that should be valid for both the running-in and steady state rubbing. Now, substituting Eq. (1) into Eq. (6) gives

$$\frac{dh}{dt} = -kpv\left(1 + e^{a(b+h)}\right) \tag{7}$$

Solving Eq. (7) with an initial condition of $h = 0$ at $t = 0$, we obtain an extended Archard equation that can be used to find wear coefficients, or to predict wear or service time if the wear coefficient is known, regardless of the material removal process duration

$$h = -\frac{1}{a}\ln\left(\left(1 + e^{ab}\right)e^{akpvt} - e^{ab}\right) \tag{8}$$

3 Experimental Details

A custom ring-on-block tribometer (Fig. 3) used here to verify the wear model in unidirectional sliding consists of a DC motor-driven spindle and a loading frame that can rotate and move radially with respect to the spindle's axis of rotation. A ring sample is fixed to the spindle's shaft and rotated with a constant speed, ω. Below the ring is a block sample bearing a protruding tooth used to provide constant contact area during the wear tests. The block is fixed to the loading frame and the tooth is pressed against the rotating ring under a constant normal load, N, which is applied by a linear actuator controlled in a closed loop using the feedback received from a normal force transducer.

The change in distance d measured by a proximity probe represents the change in a relative position between the ring and the block, which is equal to the wear depth. A friction moment, M_f, that is produced due to the sliding between the ring and the block, pushes the loading frame around the spindle's axis (needed to keep the contact area constant), but its motion is stopped by a friction force transducer to quantify the friction force, F. The effect of friction produced by a rotary bearing is canceled by a proper calibration of the force transducer.

In this work, the ring sample was made from the mild steel SAE 1045 with Vickers hardness of HV 320 and had an outer diameter of 38 mm and the average roughness, R_a, of 2.6 μm. The block samples were made from PTFE with Vickers hardness of HV 6.2 and had the tooth cross-section area of 10×2 mm^2. The steel-on-PTFE tribo-pair was chosen because it has relatively high wear rate and low stable friction [2, 26], which allows to verify conveniently the Archard wear equation within a comparatively short time.
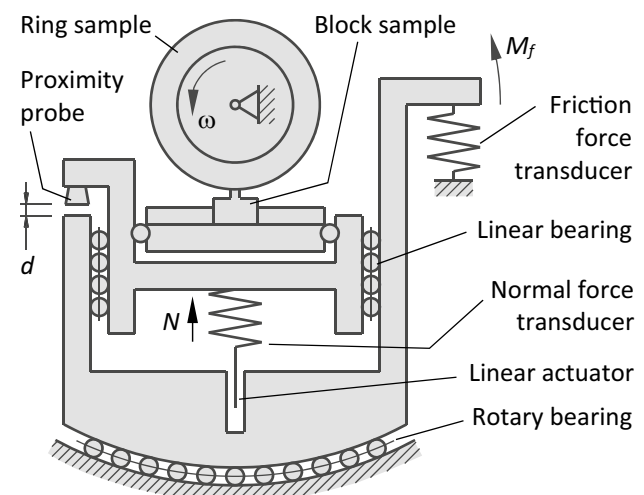

Fig. 3 Schematic of the ring-on-block tribometer

Before performing actual tests, each PTFE tooth was first ran-in to establish a conformal contact with the ring. Then, without dismounting the block sample from the rig, the tooth was ground using #220 or #320 grit SiC sandpaper wrapped around the manually and reciprocally rotated ring, while being pressed against it under the normal load of 5 N. This roughening procedure was repeated before each test. After roughening, the tested tooth was cleaned with a fresh dry residue-free wipe and profiled along its length (in parallel to the spindle's axis of rotation) using a portable stylus profiler Waveline W5 (Jenoptik, Jena, Germany). Then, the ring was cleaned with acetone and set into motion with a speed of approximately 250 or 500 rpm. The tooth was pressed against the rotating ring under the normal load of 5 or 10 N to carry out a wear test that lasted for about 3 times the running-in duration, so the samples were brought well into the steady state wear regime. This roughen-then-test sequence was repeated until the tooth was completely worn (after 4–6 consecutive runs) before mounting the next block sample. Each combination of the load, speed and initial surface finish was tested at least 4 times. The temperature and relative humidity in the lab were 23–26 °C and 30–50%, respectively.

To illustrate the bearing ratio curve approximation with logistic function, the studied surfaces were characterized using a 3D optical profiler ContourGT-I (Bruker, San Jose, CA).

4 Model Verification

Figure 4 presents the steady state coefficients of friction and wear obtained for PTFE blocks ground with two different sandpapers and pressed under two different loads against a steel ring rotating with two different speeds (in total, 8 combinations of roughness, load, and speed). The same results are shown as a function of each parameter, and as expected, both the coefficient of wear and the coefficient of friction are found to be independent of either the normal load, the sliding speed, or the initial roughness. The variances of both coefficients are predictably high [2] and their mean values ($\overline{f} = 0.25$, $\overline{K} = 3.3 \cdot 10^{-5}$) correspond to the literature data [2, 26], suggesting that these results are coherent so they can be used to verify the model.

Several illustrative examples of the evolution of wear depth plotted as a function of time are shown in Fig. 5a. The experimental results are presented as they were recorded. The model predictions were computed using Eq. (8), with the constants a and b obtained from the initial surface topography using Eqs. (2) and (3c), and the coefficient of wear k obtained from the steady state portion of each specific experiment using Eq. (5). It is obvious that there is a good match between the measured and predicted results, though the wear

depth prediction during running-in is less accurate than that during steady state, as can be seen in inset in Fig. 5a. In line with this finding, analysis of the fit quality reveals that the least (among all experiments) coefficients of determination, R^2, are 0.914 and 0.998 for the running-in ($h \leq R_t$) and steady state ($h > R_t$) portions of wear curves, respectively. Thinking about the differences between the experiment and the theory, we can possibly attribute them to (1) the fact that the representative bearing ratio curves used in calculations were obtained from the profile traces of 4.8 mm long so they could have somewhat smaller total peak-to-valley height than the real bearing ratio curves of the nominal contact area of 10×2 mm^2, (2) the use of approximated Eq. (3c), (3) neglect of surface deformation and the corresponding increase of contact area, and (4) the assumption that such complex phenomenon as running-in can be reduced to the effect of roughness only, with all other contributors, such as formation of transfer layers and loose wear particles, and chemical or physical interactions being neglected to a first approximation.

A complete data set of the measured and estimated total wear depth values is presented in Fig. 5b. Again, we can see that the match between the theory and the experiment is good, with the correlation trendline exhibiting the slope of nearly 1 calculated with the coefficient of determination of 0.998. This finally proves that the above analysis of the running-in wear is correct for at least the conditions tested here. Considering that the original Archard wear model has been verified under a wide range of conditions over the last 70 years, it is possible to assume that the extension of this model can be used to predict the wear depth with reasonable accuracy under other conditions as well. Interestingly, given that the real contact area is not needed to be known to find wear, this model indirectly suggests that the acquired (steady state) surface roughness can possibly be estimated without knowing the initial surface finish.

In addition, although it is clear from Fig. 5 that the use of logistic function to approximate the bearing ratio curve is legitimate, it would still be instructional to illustrate the quality of this approximation here. Figure 6 presents three examples of the bearing ratio curve obtained for the PTFE surfaces before and after the wear test. The curves are shown in the as measured and approximated forms, with the two approximations based on (1) the logistic function built using Eqs. (1)–(3) calibrated with the measured R_k, Mr_1, Mr_2, and $R_{pk}*$ and (2) the Gaussian distribution function calibrated with the measured root-mean-square roughness, R_q. The comparison based on plotting the relative error

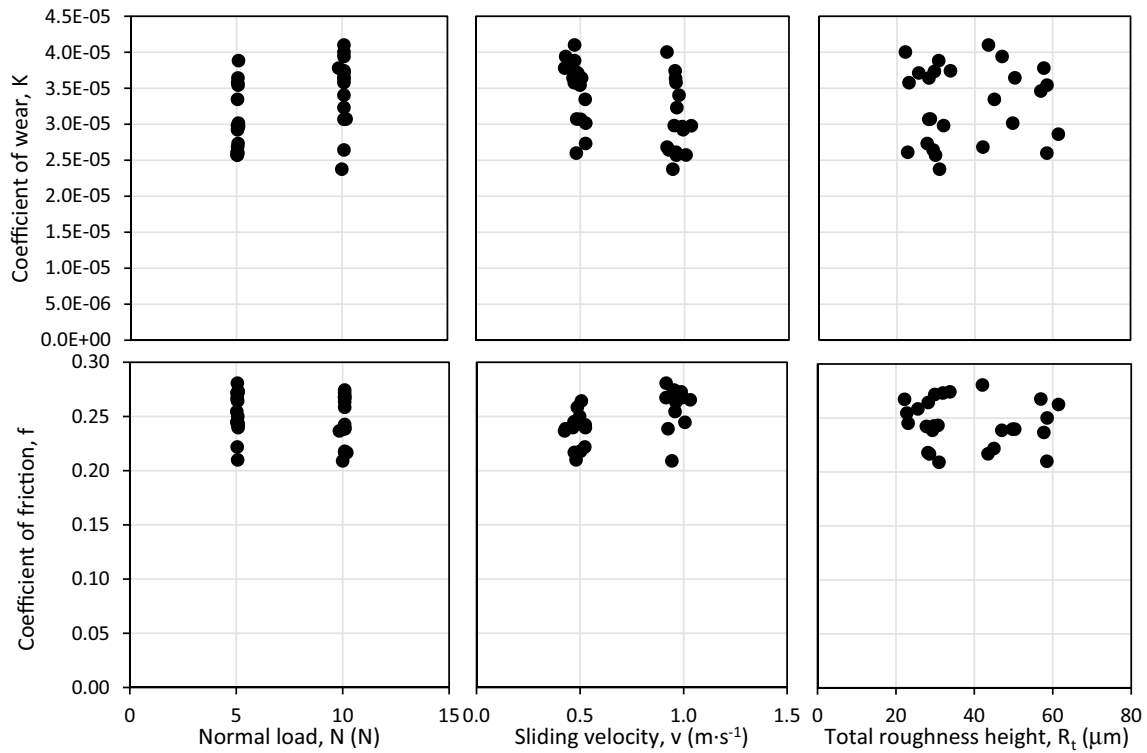$$E = \frac{|h_m - h_e|}{R_t} \cdot 100 \tag{9}$$

Fig. 4 Steady state coefficients of friction and wear of PTFE sliding against steel in dry conditions, presented as functions of normal load, sliding velocity, and initial total roughness height
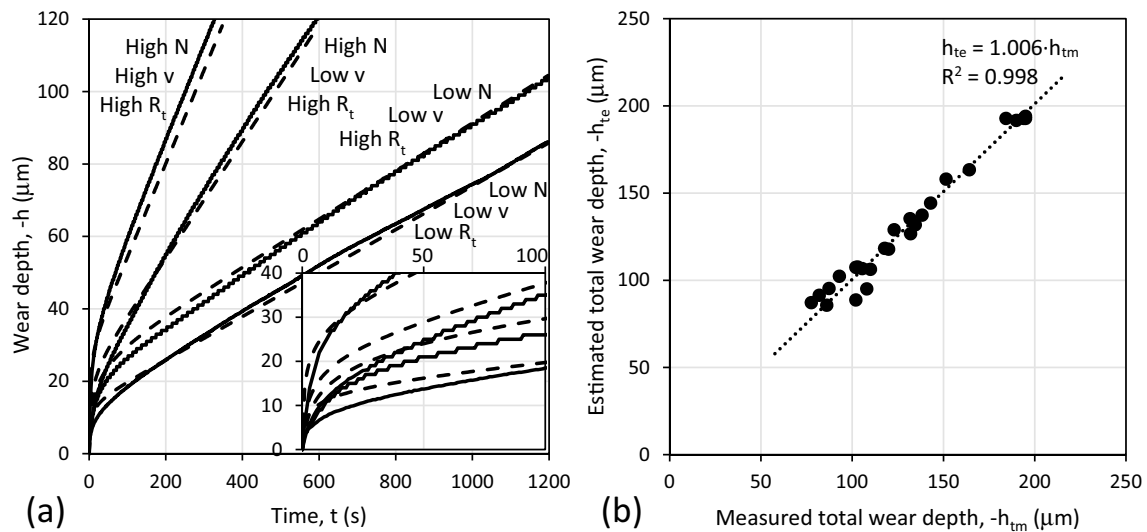

Fig. 5 a Illustrative examples of the evolution of wear depth with time. Inset represents the close-up of the running-in period. Solid lines represent experimental data, dashed lines represent the model predictions. **b** Correlation of estimated and measured total wear depth in all experiments

where h_m and h_e are the measured and estimated heights, respectively, proves that the logistic approximation is better than the widely employed Gaussian approximation. The average relative errors (for the logistic function – 0.72%, 0.95% and 0.27% and for the Gaussian function – 0.35%, 1.61% and 0.47% for Fig. 6a–c, respectively) demonstrate that the logistic approximation is about 20% more accurate than the Gaussian approximation. Though this improvement
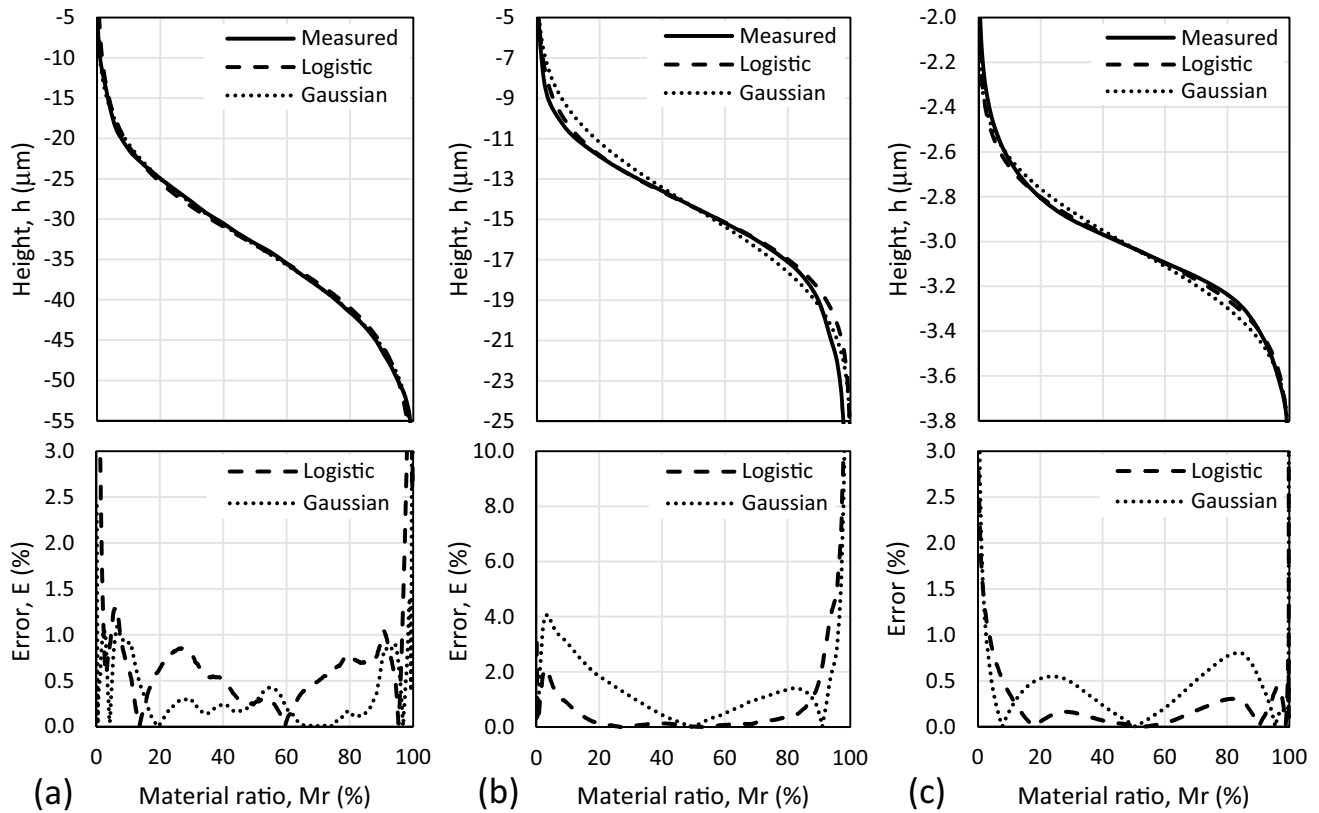
Fig. 6 Illustrative examples of the measured and approximated bearing ratio curves (along with their approximation accuracies) obtained for three PTFE surfaces that are **a** ground by #220 sandpaper, **b** ground by #320 sandpaper, and **c** worn against steel sample

in accuracy may be not significant considering that only a small deviation from the measured data is observed here with both approximations (see Fig. 6), the logistic description of rough surfaces is simpler, which can make it more attractive in engineering practice.

5 Conclusion

The results obtained in this work can be summarized to draw the following conclusions:

(1) The steady state Archard wear equation was extended into the running-in regime using the bearing ratio curve representing the initial surface topography.

(2) If the initial surface finish is defined, the extended equation can be employed (a) to evaluate the wear coefficient after measuring the wear depth only once (without the need to interrupt testing for finding intermediate values), and (b) to predict service life under given loading conditions or to determine the loading conditions

for a required service life when the wear coefficient is known.

(3) The bearing ratio curve can be efficiently approximated using the logistic function calibrated by four standard surface roughness parameters, and this approximation is found to be more accurate than the widely used Gaussian normal distribution function.

(4) Regardless of the approximation accuracy, the logistic representation of surface finish is simpler than that based on the normal distribution function and, given that the logistic function has easily calculated derivative and antiderivative, it may become useful in contact mechanics.

Data Availability The author confirms sole responsibility for the study conception and design, data collection, analysis and interpretation of results, and manuscript preparation.

Declarations

Conflict of interest The author declares that no funds, grants, or other support were received during the preparation of this manuscript. The author has no relevant financial or non-financial interests to disclose.

References

1. Archard, J.F.: Contact and rubbing of flat surfaces. J. Appl. Phys. **24**, 981–988 (1953)
2. Hutchings, I., Shipway, P.: Tribology: Friction and Wear of Engineering Materials, 2nd edn. Elsevier, Oxford (UK) (2017)
3. Varenberg, M.: Towards a unified classification of wear. Friction **1**, 333–340 (2013)
4. Feng, K., Borghesani, P., Smith, W.A., Randall, R.B., Chin, Z.Y., Ren, J., Peng, Z.: Vibration-based updating of wear prediction for spur gears. Wear **426–427**, 1410–1415 (2019)
5. Ruggiero, A., Sicilia, A.: Lubrication modeling and wear calculation in artificial hip joint during the gait. Tribol. Int. **142**, 105993 (2020)
6. Dai, L., Sorkin, V., Zhang, Y.-W.: Effect of surface chemistry on the mechanisms and governing laws of friction and wear. ACS Appl. Mater. Interfaces. **8**, 8765–8772 (2016)
7. Godet, M.: Modeling of friction and wear phenomena. In: Ling, F.F., Pan, C.H.T. (eds.) Approaches to Modeling of Friction and Wear, pp. 12–36. Springer, New York
8. Yuan, H., Song, J., Schinow, V.: Simulation methodology for prediction of the wear on silver-coated electrical contacts with a sphere/flat configuration. IEEE Transactions on Components, Packaging and Manufacturing Technology **8**, 364–374 (2018)
9. Queener, C.A., Smith, T.C., Mitchell, W.L.: Transient wear of machine parts. Wear **8**, 391–400 (1965)
10. Zhang, Y., Kovalev, A., Hayashi, N., Nishiura, K., Meng, Y.: Numerical prediction of surface wear and roughness parameters during running-In for line contacts under mixed lubrication. J Tribol (2018). https://doi.org/10.1115/1.4039867
11. Gu, C., Zhang, D.: Modeling and prediction of the running-in behavior of the piston ring pack system based on the stochastic surface roughness. Proceedings of the Institution of Mechanical Engineers, Part J: Journal of Engineering Tribology **233**, 1857–1877 (2019)
12. Winkler, A., Marian, M., Tremmel, S., Wartzack, S.: Numerical modeling of wear in a thrust roller bearing under mixed elastohydrodynamic lubrication. Lubricants **8**, 58 (2020)
13. Greenwood, J.A., Williamson, J.B.P.: Contact of nominally flat surfaces. Proc. R. Soc. Lon. Ser. A **295**, 300–319 (1966)
14. Kogut, L., Etsion, I.: A finite element based elastic-plastic model for the contact of rough surfaces. Tribol. T. **46**, 383–390 (2003)
15. Jackson, R.L., Green, I.: A statistical model of elasto-plastic asperity contact between rough surfaces. Tribol. Int. **39**, 906–914 (2006)
16. Ghosh, A., Sadeghi, F.: A novel approach to model effects of surface roughness parameters on wear. Wear **338–339**, 73–94 (2015)
17. Pawar, G., Pawlus, P., Etsion, I., Raeymaekers, B.: The effect of determining topography parameters on analyzing elastic contact between isotropic rough surfaces. J. Tribol. **135**, 011401 (2013)
18. Fecske, S.K., Gkagkas, K., Gachot, C., Vernes, A.: Interdependence of amplitude roughness parameters on rough Gaussian surfaces. Tribol. Lett. **68**, 43 (2020)
19. Green, I.: Exact spectral moments and differentiability of the Weierstrass-Mandelbrot fractal function. J. Tribol. **142**, 041501 (2020)
20. Abbott, E.J., Firestone, F.A.: Specifying surface quality: a method based on accurate measurement and comparison. ASME Mech. Engr. **55**, 569–572 (1933)
21. Kumar, R., Prakash, B., Sethuramiah, A.: A systematic methodology to characterise the running-in and steady-state wear processes. Wear **252**, 445–453 (2002)
22. Astakhov, V.P., Davim, J.P.: Tools Geometry and Material and Tool Wear. In: Machining: Fundamentals and Recent Advances, pp. 29–57. Springer, London, London (2008)
23. Bowden, F.P., Tabor, D.: Mechanism of metallic friction. Nature **150**, 197–199 (1942)
24. Jia, X., Grejtak, T., Krick, B., Vermaak, N.: Design of composite systems for rotary wear applications. Mater. Des. **134**, 281–292 (2017)
25. Bacaër, N.: Verhulst and the logistic equation (1838). In: A Short History of Mathematical Population Dynamics, pp. 35–39. Springer, London, London (2011)
26. Archard, J.F., Hirst, W.: The wear of metals under unlubricated conditions. Proc. R. Soc. Lon. Ser. **236**, 397–410 (1956)